AMERICAN SOCIETY FOR MICROBIOLOGY | Journal of Virology®

VIRUS-CELL INTERACTIONS

CD46 Isoforms Influence the Mode of Entry by Human Herpesvirus 6A/B in T Cells

Litten Sørensen Rossen,[a] Vivien R. Schack,[a] Katrine Kyd Holstein Thuesen,[a]* Bettina Bundgaard,[a] Per Höllsberg[a]

[a]Department of Biomedicine, Aarhus University, Aarhus, Denmark

Litten Sørensen Rossen and Vivien R. Schack contributed equally to this article. Author order was determined alphabetically.

ABSTRACT CD46 is a receptor for human herpesvirus 6A (HHV-6A) and is in some cells also important for infection with HHV-6B. CD46 has several isoforms of which the most commonly expressed can be distinguished by expression of a BC domain or a C domain in a serine-threonine-proline-rich (STP) extracellular region. Using a SupT1 CD46 CRISPR-Cas9 knockout model system reconstituted with specific CD46 isoforms, we demonstrated that HHV-6A infection was more efficient when BC isoforms were expressed as opposed to C isoforms, measured by higher levels of intracellular viral transcripts and recovery of more progeny virus. Although the B domain contains several *O*-glycosylations, mutations of Ser and Thr residues did not prevent infection with HHV-6A. The HHV-6A infection was blocked by inhibitors of clathrin-mediated endocytosis. In contrast, infection with HHV-6B was preferentially promoted by C isoforms mediating fusion-from-without, and this infection was less affected by inhibitors of clathrin-mediated endocytosis. Taken together, HHV-6A preferred BC isoforms, mediating endocytosis, whereas HHV-6B preferred C isoforms, mediating fusion-from-without. This demonstrates that the STP region of CD46 is important for regulating the mode of infection in SupT1 cells and suggests an epigenetic regulation of the host susceptibility to HHV-6A and HHV-6B infection.

IMPORTANCE CD46 is the receptor used by human herpesvirus 6A (HHV-6A) during infection of T cells, but it is also involved in infection of certain T cells by HHV-6B. The gene for CD46 allows expression of several variants of CD46, known as isoforms, but whether the isoforms matter for infection of T cells is unknown. We used a genetic approach to delete CD46 from T cells and reconstituted them with separate isoforms to study them individually. We expressed the isoforms known as BC and C, which are distinguished by the potential inclusion of a B domain in the CD46 molecule. We demonstrate that HHV-6A prefers the BC isoform to infect T cells, and this occurs predominantly by clathrin-mediated endocytosis. In contrast, HHV-6B prefers the C isoform and infects predominantly by fusion-from-without. Thus, CD46 isoforms may affect susceptibility of T cells to infection with HHV-6A and HHV-6B.

KEYWORDS CD46, HHV-6A, HHV-6B

Human herpesviruses (HHVs) enter the host cell by different entry mechanisms (1). HHV-6A and HHV-6B belong to two separate species within the *Betaherpesvirinae* subfamily. Although both of them may infect T cells, their mechanisms of infection are poorly understood. HHV-6A has been described to enter by endocytosis, using lipid raft-dependent entry or fusion-from-without (FFWO) (2–4). The entry mechanism of HHV-6B is less studied, but it has been described to enter by FFWO in certain cell lines (e.g., SupT1 and MT4 cells) (2, 5, 6).

The complement regulating protein CD46 is the receptor for HHV-6A and in some cases for HHV-6B (6). Infection with HHV-6A requires binding to CD46 (reviewed in reference 7), is blocked by antibodies to CD46 (6), and is absent in human T cells lacking

Editor Lori Frappier, University of Toronto

Address correspondence to Vivien R. Schack, vs@biomed.au.dk, or Per Höllsberg, ph@biomed.au.dk.

*Present address: Katrine Kyd Holstein Thuesen, Departments of Clinical Medicine and Dermatology, Aarhus University Hospital, Aarhus, Denmark.

The authors declare no conflict of interest.

Received 22 September 2021
Accepted 26 December 2021
Accepted manuscript posted online 12 January 2022
Published 9 March 2022

CD46 (8). In contrast, HHV-6B has significantly less avidity for CD46 and appears to use alternative receptors, such as CD134 (9, 10), a molecule that is virtually absent on resting T cells but is upregulated upon activation. However, HHV-6B may also infect cells lacking CD134, suggesting a greater promiscuity compared with HHV-6A infection (8, 11). Recent data demonstrate that other proteins, such as the tetraspanin protein CD9 (8), may modulate the infection by CD46, since both proteins together with β1-integrins are members of a microdomain that affects membrane reorganization during viral entry (12–14).

Intriguingly, CD46 is also a receptor for multiple other pathogens, including *Neisseria meningitidis*, *Neisseria gonorrhoeae*, *Streptococcus pyogenes*, measles morbillivirus, and certain species of mastadenovirus (15). The gene for CD46 is located on chromosome 1 in a cluster of complement regulators and has 14 exons that allow expression of several CD46 isoforms. The first six exons encode a signal peptide and four short consensus repeats (SCRs). The structure of SCR1 to SCR4 resembles a hockey stick with a linear arrangement of SCR1 to SCR3 and a bend between SCR3 and SCR4, positioning SCR4 in a kinked angle to the adjacent SCR domains (16). During infection, HHV-6A interacts with SCR2 and SCR3 (17), but the precise motif has not been identified.

The following three exons encode a serine-threonine-proline-rich (STP) region named by the letters A, B, and C according to the respective exons that contribute to the domain. Usually, the A domain in STP is spliced out, whereas the C domain is maintained. The B domain may or may not be spliced out. The STP region contains several predicted *O*-glycosylation sites. This region is speculated to confer interactions with ligands or other membrane proteins. It may also serve as a linker, possibly in connection with the U domain between the STP and the transmembrane domain.

The last two exons encode cytoplasmic tails 1 and 2 (Cyt1 and Cyt2), one of which is selected by alternative splicing. In general, the majority of protein isoforms share less than 50% of their interactions and tend to behave more like distinct proteins than minor variants of each other (18). Although different CD46 isoforms are expressed simultaneously, it is often ignored how this may diversify the function of CD46. It has been suggested that the two different cytoplasmic tails exert opposite functions in controlling the immune system. It appears that Cyt1 regulates the interferon-γ (IFN-γ) and interleukin 10 (IL-10) response (19, 20), and Cyt2 might function to subsequently downregulate it. In agreement with this notion, the relative expression of Cyt2 is increased following activation of T cells (21).

Atkinson's group determined that predominantly four isoforms of CD46 are expressed on the cell surface, named by their STP domains and cytoplasmic tail as BC1, BC2, C1, and C2 (22). Although an individual's expression pattern is similar in different immune cells (23), splicing in certain tissues may generate isoforms that diverge from the main pattern (24).

Whereas the splicing of Cyt tails may affect regulation of the immune system, it is possible that the splicing of the extracellular STP domain affects ligand binding or entry. Although all of the CD46-binding pathogens are dependent on one or more of the four SCR, *Neisseria* spp. are also dependent on the STP domain (25). To address whether the extracellular STP domain is important for HHV-6A or possibly HHV-6B infection, we expressed CD46 isoforms in CRISPR-Cas9-edited T cells lacking CD46, specifically addressing a potential role of the B domain for infection by HHV-6A and HHV-6B. We used a SupT1 cell line model, since CD46 is required for both HHV-6A and HHV-6B infection of the SupT1 cell line (8).

RESULTS

Establishment of T-cell lines with stable expression of individual CD46 isoforms. In the present study, we used the previously described CD46 knockout SupT1 cell line, named SupT1$^{\Delta CD46}$ (8), as a background for the generation of various stable cell lines expressing specific CD46 isoforms, denoted SupT1^{BC1}, SupT1^{BC2}, SupT1^{C1}, and SupT1^{C2} (Fig. 1A). We succeeded in isolating cell lines displaying very similar surface levels of CD46: SupT1$^{BC1.1}$,

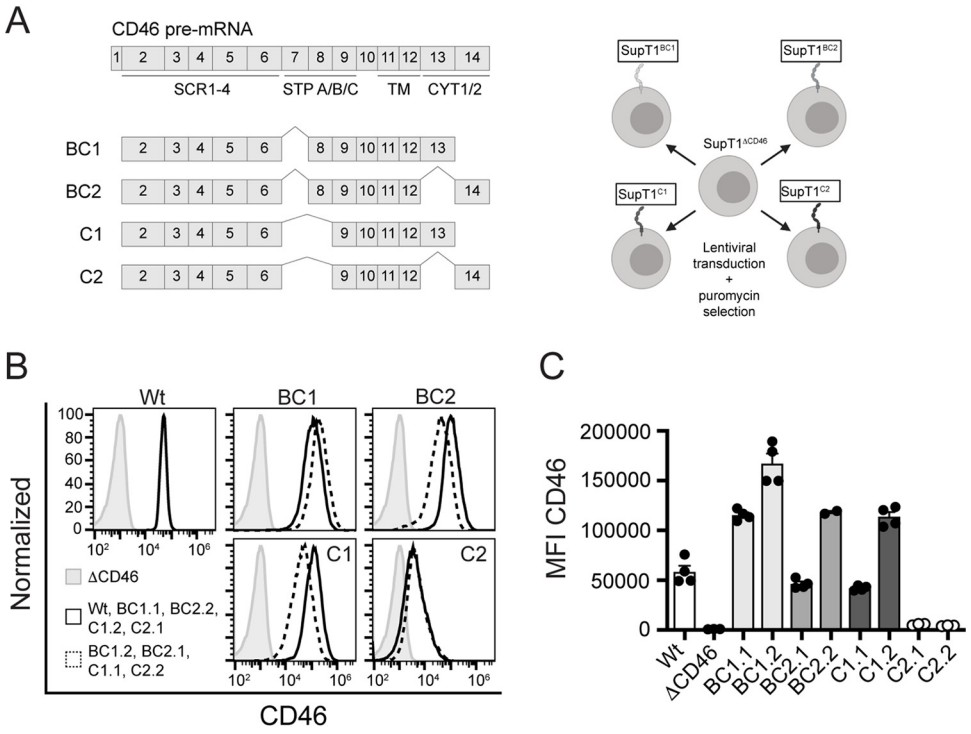

FIG 1 Generation of stable SupT1 cell lines expressing separate CD46 isoforms. (A) Graphical illustration showing the organization of the mRNA for the four most commonly expressed CD46 isoforms and an illustration of the model system established. The figure was created with Biorender.com software. (B) Flow cytometry analysis illustrating the surface expression of CD46 on the separate SupT1 cell lines. The separate names (BC1.1/BC1.2) represent the separate cell lines isolated after transduction with different amounts of the respective lentivirus preparation. The cell lines BC1.1, BC2.2, and C1.2 express a similar CD46 surface level. The histogram for SupT1$^{\Delta CD46}$ is included for comparison (shown in gray). (C) Bar graph of the median fluorescence intensity (MFI) of CD46-PE in isoform-expressing SupT1 cell lines. The data show independent experiments with the mean ± standard error of the mean (SEM) indicated. SCR, short consensus repeat; STP, serine-threonine-proline-rich region; Wt, wild type; TM, transmembrane.

SupT1$^{BC2.2}$, and SupT1$^{C1.2}$ (Fig. 1B and C). Stable CD46 expression was verified on a regular basis using flow cytometry. Of note, despite several attempts, we were unable to obtain a SupT1^{C2} cell line expressing CD46 at a level comparable to the other cell lines (Fig. 1B and C).

HHV-6A$_{GS}$ and HHV-6B$_{Z29}$ employ separate CD46 isoforms for infection. To investigate whether the CD46 isoforms were equal in mediating infection by HHV-6A$_{GS}$ and HHV-6B$_{Z29}$, we infected the CD46-expressing cells and quantified the level of U81 and U23 viral transcripts 24 h postinfection (hpi) by real-time PCR analyses (Fig. 2A and B). U81 and U23 have previously been described as immediate early (IE) and late (L) genes and belonging to groups 2 and 4, respectively, of a total of 6 groups that classify the genes according to their kinetic expression (26).

Noticeably, despite a similar CD46 surface expression, the level of viral infection depended on the individual isoform. HHV-6A$_{GS}$ infection was found to be promoted in cell lines expressing BC isoforms, whereas the C1 isoform promoted HHV-6B$_{Z29}$ infection. When comparing cells with similar CD46 surface expression, a 1.7-fold increase was demonstrated in the U23 mRNA level upon HHV-6A$_{GS}$ infection of BC1-expressing cells compared with C1-expressing cells (95% CI, 1.23 to 2.32; $P = 0.029$) (Fig. 2A), whereas a 3.5-fold increase was demonstrated in the U23 mRNA level of HHV-6B$_{Z29}$ in C1-expressing cells compared with BC1-expressing cells (95% CI, 2.63 to 4.69; $P = 0.008$) (Fig. 2B). Similar data were obtained using U81 as a measure of infection.

For the subsequent experiments, we used SupT1$^{BC1.1}$, SupT1$^{BC2.2}$, and SupT1$^{C1.2}$ that all had comparable levels of CD46 expression. To investigate the role of the CD46 STP B domain for binding of HHV-6A$_{GS}$, we used the viral glycoprotein gp60/110 as a measure of viral binding to the cell. SupT1^{C1} cells displayed 32 and 35% less gp60/110

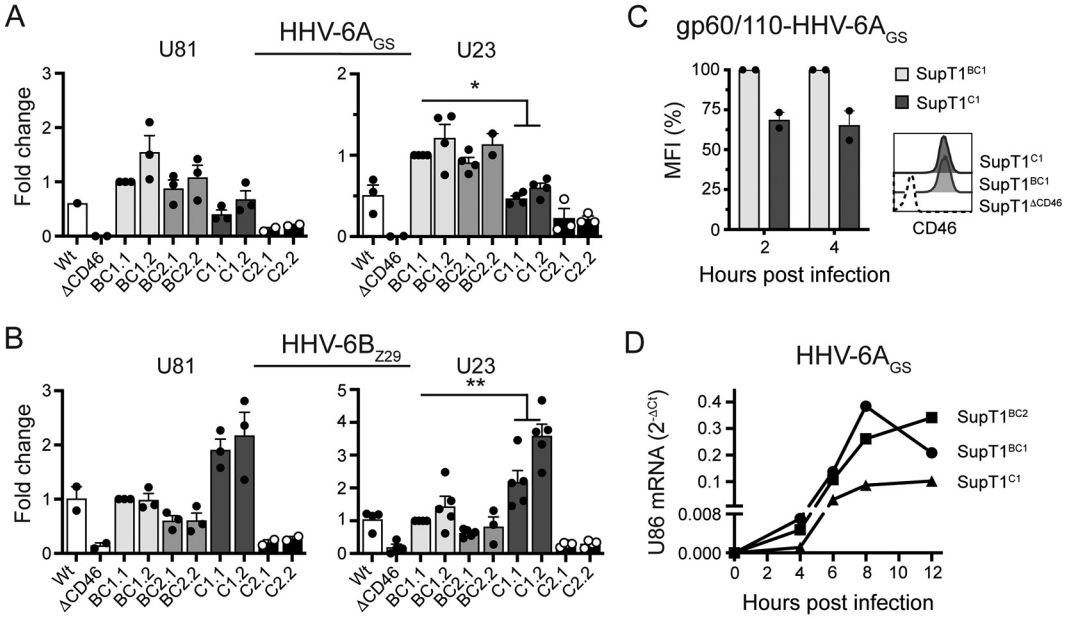

FIG 2 BC-expressing isoforms favor human herpesvirus 6A (HHV-6A$_{GS}$) infection, and C1-expressing isoforms favor HHV-6B$_{Z29}$ infection. (A, B) The isoform-expressing SupT1 cell lines were incubated with HHV-6A$_{GS}$ or HHV-6B$_{Z29}$ for 24 h, and the infection was assessed by real-time PCR analysis of the level of viral transcripts U81 and U23 at 24 h postinfection (hpi). The data represent $2^{-\Delta\Delta CT}$ (fold change) from individual experiments presented as means ± SEM, with normalization to SupT1$^{BC1.1}$. *, $P < 0.05$; **, $P < 0.01$ (Mann-Whitney test). (C) Flow cytometry analysis of viral gp60/110 adsorption to the cell surface, determined at 2 and 4 hpi following infection with HHV-6A$_{GS}$. The data represent the mean fluorescence intensity (MFI) values for cells treated with 0.1% sodium azide 30 min prior to incubation with virus, shown as percentages of the SupT1^{BC1} cell line. The histograms are representative for the respective CD46 expression, verifying a similar expression level on SupT1$^{BC1.1}$ and SupT1$^{C1.2}$ prior to infection. (D) Real-time PCR analysis of the level of viral transcript U86 at the indicated time points. The results are shown as $2^{-\Delta CT}$, from one representative of three independent experiments.

adsorption at 2 and 4 hpi, respectively, compared with SupT1^{BC1} cells. (Fig. 2C). The observed increase in binding of HHV-6A$_{GS}$ to the SupT1^{BC1} cells could not be explained by an increase in CD46 expression, and therefore the data indicate that the B domain is important for the receptor binding of HHV-6A$_{GS}$.

In order to assess infection after binding, we investigated the level of the IE viral transcript U86 at various early time points upon infection with HHV-6A$_{GS}$ (Fig. 2D). The level of U86 transcript was increased in both SupT1^{BC1} and SupT1^{BC2} compared with the SupT1^{C1} cell line. The levels of U86 mRNA determined in SupT1^{BC1} were on average 2.7- and 2.4-fold higher at 6 and 8 hpi, respectively, compared with the SupT1^{C1} cell line. At 4 hpi, the level of U86 mRNA was barely detectable for SupT1^{C1}-infected cells, whereas both SupT1^{BC1} and SupT1^{BC2} displayed levels clearly above the detection limit (Fig. 2D). These results strongly suggest a role for the B domain in the infection process of HHV-6A$_{GS}$.

The CD46 isoform B domain differentially affects infection with HHV-6A$_{GS}$ and HHV-6B$_{Z29}$. Human cells express more than one CD46 isoform. Since our data indicate an HHV-6A$_{GS}$ preference for the BC1 isoform, whereas HHV-6B$_{Z29}$ preferred the C1 isoform, we speculated that coexpressing a less or more favorable CD46 isoform would modulate the efficiency of infection. To address this, we generated a stable SupT1 cell line, expressing both the C1 and the BC1 isoforms of CD46, named SupT1$^{C1/BC1}$, with a CD46 surface expression level comparable with the previously established SupT1^{BC1} and SupT1^{C1} cell lines (Fig. 3A and B). The SupT1^{wt} displayed C1 and C2 expression of about 30% of total CD46 mRNA each, whereas the mRNA level of the BC1 and BC2 isoforms corresponded to approximately 20% each (Fig. 3C). In the SupT1$^{C1/BC1}$, the amount of mRNA was found to be approximately 40% BC1 and 60% C1 (Fig. 3D). Infection with HHV-6A$_{GS}$ and HHV-6B$_{Z29}$ demonstrated that the SupT1$^{C1/BC1}$ cell line displayed HHV-6A$_{GS}$ and HHV-6B$_{Z29}$ U86 mRNA levels between those determined for SupT1^{BC1} and SupT1^{C1}

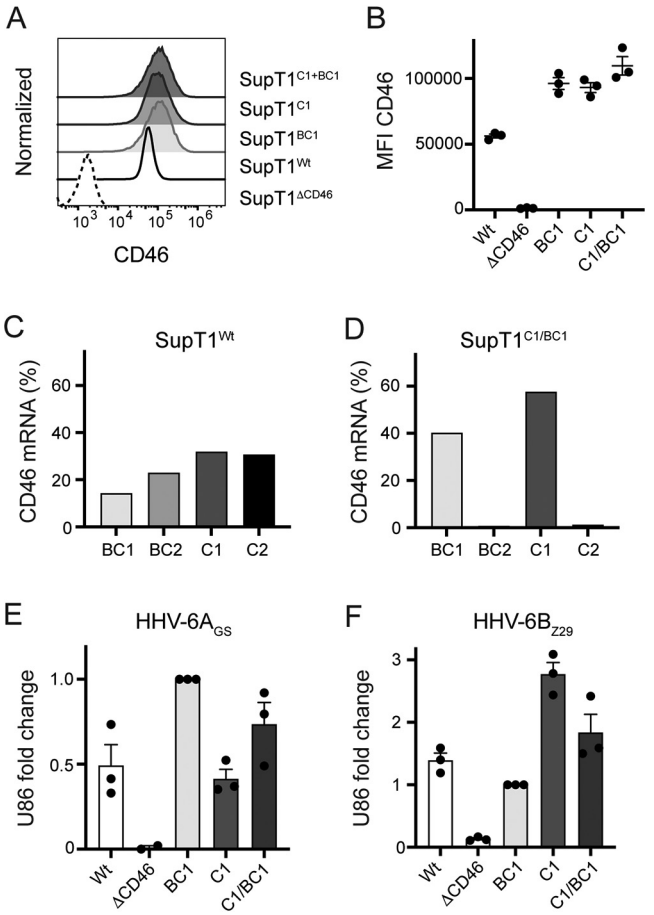

FIG 3 Coexpression of BC1 and C1 affects the susceptibility of HHV-6A and HHV-6B. (A) Flow cytometry analysis of CD46 surface expression with representative histograms for the separate cell lines prior to infection. (B) CD46-PE median fluorescence intensity (MFI). Real-time PCR analysis of the separate CD46 isoforms in (C) SupT1^{wt} and (D) SupT1$^{C1/BC1}$, shown as percentages of the total CD46 mRNA expression level from one representative experiment. (E, F) The level of HHV-6A$_{GS}$ and HHV-6B$_{Z29}$ infection at 7 hpi, characterized by analysis of the relative expression of IE transcript U86. The data represent the fold change (i.e., $2^{-\Delta\Delta CT}$) relative to the SupT1^{BC1}, presented as the means ± SEM of three independent experiments.

(Fig. 3E and F), which is in line with our previous findings and thus supports the notion that HHV-6A prefers BC1 over C1 and HHV-6B prefers C1 over BC1.

The B domain of CD46 affects the production of progeny virus. We wondered whether the observed difference in the CD46 isoform dependency during early infection would translate to different amounts of viral particles being produced. To investigate this, supernatants from SupT1^{BC1} and SupT1^{C1} were collected at various time points after infection with HHV-6A$_{GS}$ and HHV-6B$_{Z29}$, respectively, and analyzed for the amount of viral DNA (Fig. 4). The level of viral DNA correlated with the results of mRNA transcripts, displaying HHV-6A$_{GS}$ preference for the BC1 and HHV-6B$_{Z29}$ preference for the C1 isoform. At 96 hpi, the HHV-6A$_{GS}$ infection of SupT1^{BC1} cells gave rise to a 3.4-fold increase in viral U7 DNA compared with the SupT1^{C1} cell line (Fig. 4A). Likewise, the HHV-6B$_{Z29}$ infection of SupT1^{C1} cells gave rise to a 6.9-fold increase in viral U7 DNA at 96 hpi compared with the U7 level measured in the supernatant of the SupT1^{BC1} cell line (Fig. 4C). Quantification of the DNA level of U81 and U86 gave similar results, as observed for U7 DNA (Fig. 4B and D). All experiments showed the same trend, with BC1 favoring HHV-6A$_{GS}$ infection and C1 favoring HHV-6B$_{Z29}$ infection. Taken together, the data support the previous findings and demonstrate that the production of progeny viral particles for both HHV-6A$_{GS}$ and HHV-6B$_{Z29}$ is influenced by the isoform of CD46.

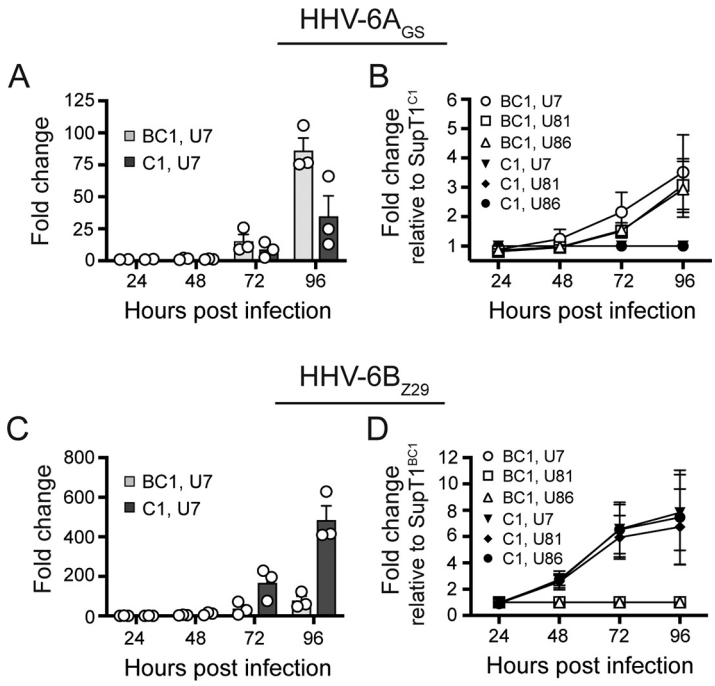

FIG 4 The presence of the B domain leads to higher level of HHV-6A DNA, whereas its exclusion promotes production of HHV-6B. SupT1$^{BC1.1}$ and SupT1$^{C1.2}$ cell lines were infected with HHV-6A$_{GS}$ (A, B) or HHV-6B$_{Z29}$ (C, D) for 24, 48, 72, and 96 h. The nucleic acids were purified from the collected supernatants and analyzed by real-time PCR. (A, C) Bar charts with individual measurements illustrating the increase of U7 DNA over time, represented as fold change (i.e., $2^{-\Delta\Delta CT}$), normalized to the mean Ct value for HHV-6A$_{GS}$- and HHV-6B$_{Z29}$-infected SupT1^{BC1} cells at 24 hpi, respectively. The bars represent the means ± SEM. (B, D) Fold change of U7, U81, and U86 (i.e., $2^{-\Delta\Delta CT}$). The Ct values of the separate time points are normalized to the respective value obtained for SupT1^{C1} for HHV-6A$_{GS}$-infected cells (i.e., $2^{-\Delta CT(BC1/C1) - \Delta CT(C1)}$) or SupT1^{BC1} for HHV-6B$_{Z29}$-infected cells (i.e., $2^{-\Delta CT(BC1/C1) - \Delta CT(BC1)}$). The graphs represents the mean values ± SEM of three independent experiments, except data for HHV-6A$_{GS}$-infected cells at 24 h, which consist of two independent experiments.

***O*-Glycosylations within the B domain are not required for HHV-6A$_{GS}$ infection.** The presence of a B domain increases the molecular mass by approximately 8 kDa (Fig. 5A) (27). The B domain is *O*-glycosylated (22), which might influence HHV-6A$_{GS}$ binding and entry. To investigate the impact of *O*-glycosylation, we mutated putative glycosylation sites in the B domain to alanine residues, generating six mutated variants of BC1 (i.e., STP mutants m1 to m6) (Fig. 5B). The CD46 glycosylation level of the separate cell lines was characterized by Western blotting analyses showing distinct differences in the migration patterns of the individual STP mutants (Fig. 5C). Notably, SupT1^{m2}, SupT1^{m3}, and SupT1^{m6} displayed a reduction in the molecular mass compared with SupT1^{BC1}, thus indicating that at least one of the threonines T288, T291, and T292 was glycosylated (Fig. 5C). In contrast, the migration of CD46 from cells of SupT1^{m1}, SupT1^{m4}, and SupT1^{m5} resembled SupT1^{BC1}, indicating that the targeted serines in these variants (S287, S289, S290, S294, S297, S298, and S300) did not constitute glycosylation sites in SupT1 cells. Flow cytometry analysis demonstrated an increased CD46 expression level for the SupT1$^{m1\text{-}m5}$ cell lines and a somewhat reduced CD46 expression level in the SupT1^{m6} cells compared with SupT1^{BC1} (Fig. 5D). Nevertheless, HHV-6A$_{GS}$ infection of the cell lines as measured by U81 and U86 viral transcripts at 8 hpi (Fig. 5E) resulted in similar levels of infection. Since the STP mutants displayed various CD46 expression levels, we cannot exclude a minor contributing role for the targeted glycosylation sites in mediating entry of HHV-6A$_{GS}$. Our data do show, however, that the targeted glycosylation sites are dispensable for HHV-6A$_{GS}$ infection.

The entry mechanisms of HHV-6A and HHV-6B are affected by CD46 isoforms. The preference for separate isoforms during the early steps of infection suggested the possibility that HHV-6A$_{GS}$ and HHV-6B$_{Z29}$ may enter cells by separate mechanisms. In

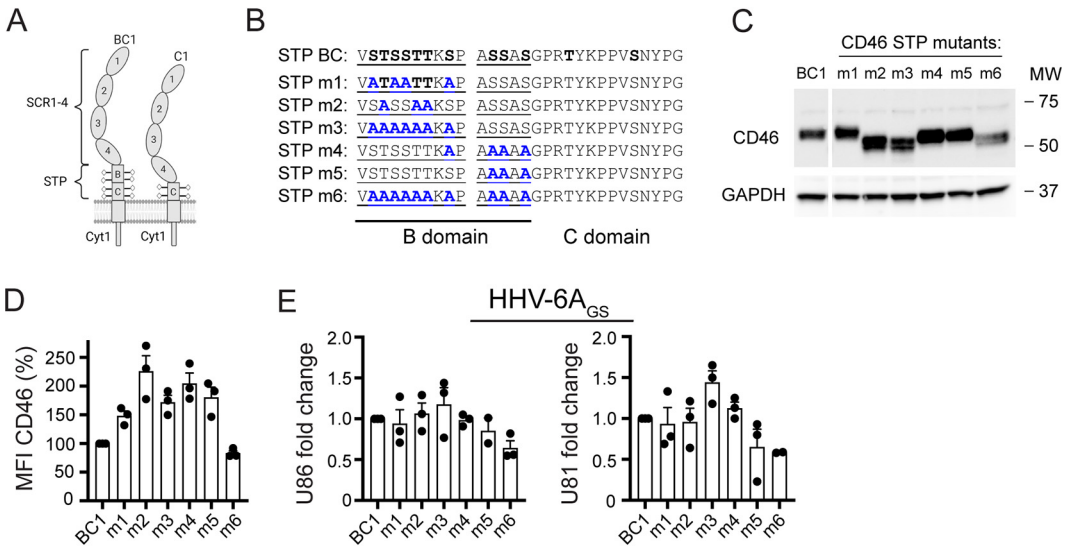

FIG 5 *O*-Glycosylations in the B domain do not contribute to HHV-6A$_{GS}$ infection. (A) Schematic illustration of the CD46 isoforms BC1 and C1. The figure was created with Biorender.com software. (B) Illustration of the amino acid sequence of the CD46 BC domain with indications of the putative *O*-glycosylation sites in bold. The STP mutants m1 to m6 are shown with the separate alanine substitutions highlighted in blue. (C) Western blotting of cell lysates from SupT1^{BC1} (BC1) and STP mutants m1 to m6. GAPDH is used as a loading control. (D) Flow cytometry analysis of CD46 surface expression on m1 to m6. The graph represents the MFI values, shown as percentages of the SupT1^{BC1} (BC1) cell line, with the bars indicating the means ± SEM of three independent experiments. (E) HHV-6A$_{GS}$ infection at 8 hpi. The data represent fold change in expression levels of U86 and U81 (i.e., $2^{-\Delta\Delta CT}$) relative to the SupT1^{BC1} cell line, with the bars indicating the means ± SEM of three independent experiments. GAPDH, glyceraldehyde-3-phosphate dehydrogenase; MW, molecular weight.

order to assess this possibility, the cellular uptake of virus by clathrin-mediated endocytosis was inhibited using three different endocytosis inhibitors targeting the internalization in distinctive ways (Fig. 6A).

Overall, the cell lines tolerated the inhibitors well within the short time of the experiment. Only small variations in viability were observed for chloroquine-treated HHV-6B-infected cells and dynasore-treated HHV-6A-infected SupT1^{Wt} cells (Fig. 6B to D, right column). To rule out that the inhibitors altered the level of CD46 during infection, the CD46 expression was examined at 2 and 4 h of treatment with 50 μM chloroquine, 50 μM dynasore, and 25 μM chlorpromazine. None of the inhibitors affected CD46 expression at these time points (data not shown).

For HHV-6A$_{GS}$-infected cells, all inhibitors led to a concentration-dependent reduction in the level of U86 mRNA transcripts in SupT1^{wt}, SupT1^{BC1}, and SupT1^{C1} 7 hpi (Fig. 6B to D). In comparison, the presence of endocytosis inhibitors affected the HHV-6B$_{Z29}$ infection differently (Fig. 6B to D). The viral gene expression in HHV-6B$_{Z29}$-infected SupT1^{C1} cells was not inhibited by the lower concentrations of chlorpromazine, whereas it was increased by chloroquine treatment and inhibited by dynasore, however with diminishing effect at increasing concentrations. In contrast, viral gene expression in HHV-6B$_{Z29}$ infection of the SupT1^{BC1} cells was markedly affected by all the inhibitors, displaying a concentration-dependent inhibition, most evident by chlorpromazine treatment but also observed after chloroquine treatment.

These results are consistent with the interpretation that the entry mechanism through BC1 occurs mainly by clathrin-mediated endocytosis, because all inhibitors significantly affected this pathway for both HHV-6A and HHV-6B. In contrast, the C1-mediated entry was less affected by these inhibitors during HHV-6B infection, suggesting that C1 expression allows a different entry mechanism.

To further explore whether the preference for the C1-mediated entry was associated with a different entry mechanism, virus-induced FFWO was investigated. SupT1 cells were incubated with either CellTrace Violet (CTV) or CellTrace Far Red (CTR) and

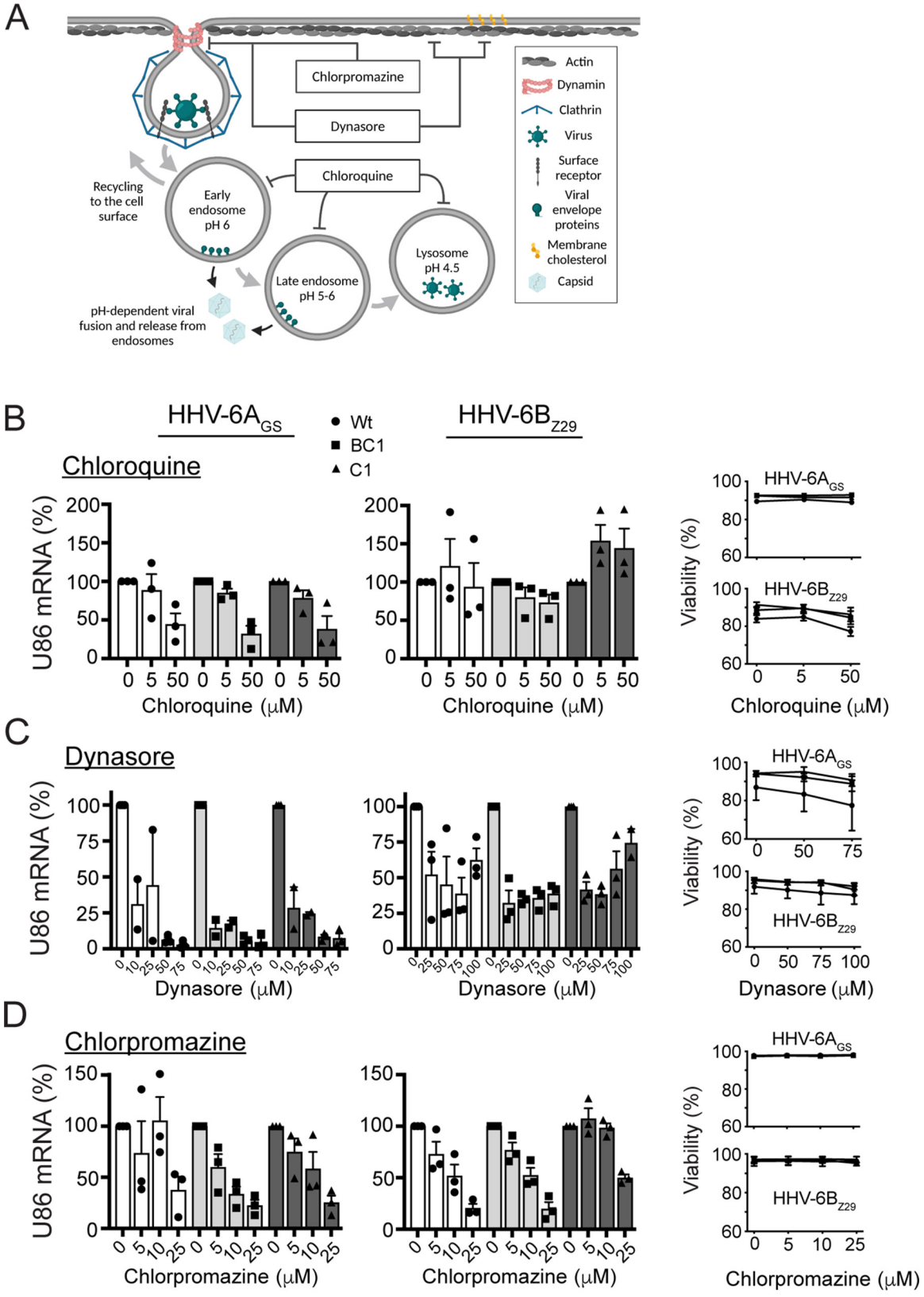

FIG 6 Entry via the BC isoform is inhibited more efficiently by clathrin-mediated endocytosis inhibitors than entry via the C1 isoform. (A) Schematic illustration summarizing clathrin-mediated endocytosis of virus leading to cell entry or lysosomal degradation. Some of the cellular effects of chloroquine, dynasore, and chlorpromazine are illustrated. The figure was created with Biorender.com software. (B to D) The CD46 isoform-specific SupT1 cell lines SupT1^{wt}, SupT1^{BC1} (BC1.1), and SupT1^{C1} (C1.2) were treated with the indicated

(Continued on next page)

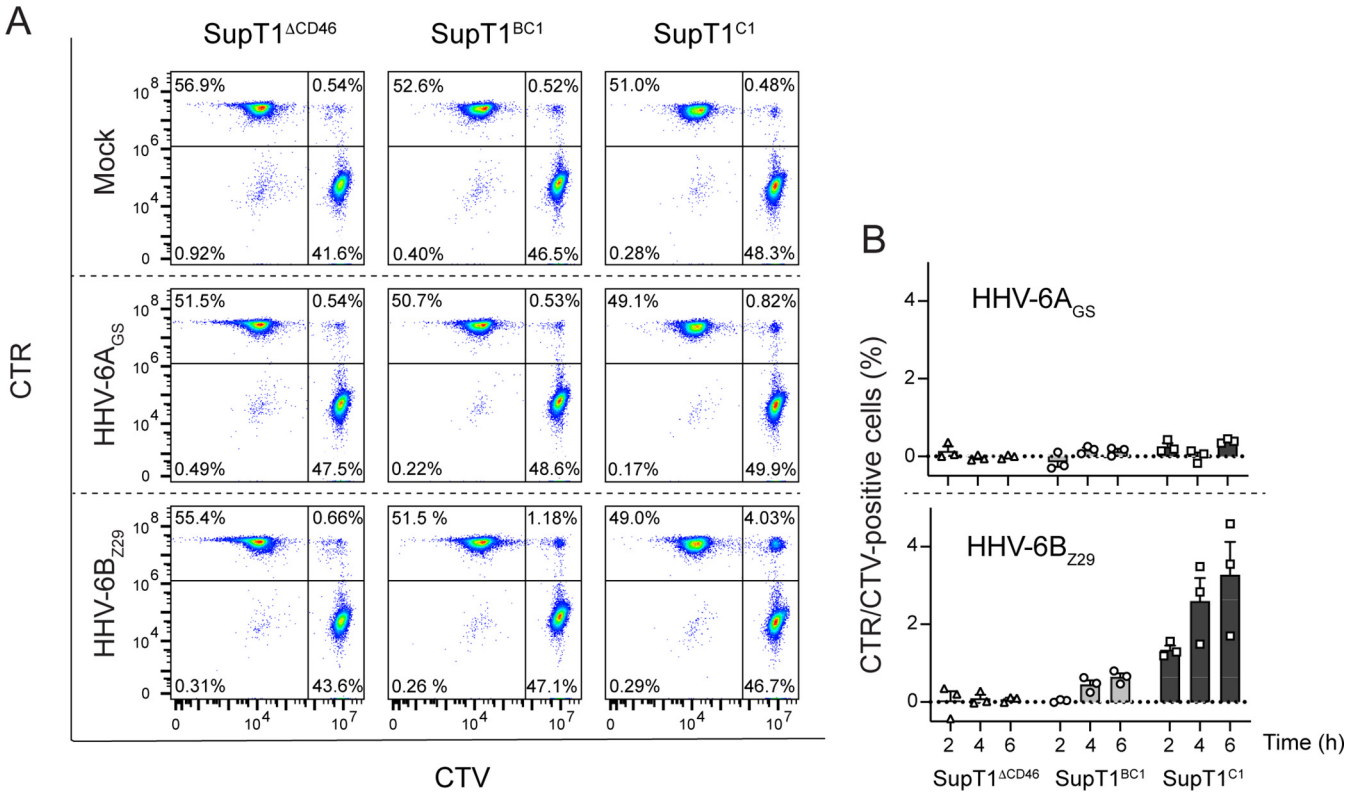

FIG 7 The C1 isoform supports cell-cell fusion by infection with HHV-6B$_{Z29}$ but not HHV-6A$_{GS}$. SupT1$^{\Delta CD46}$, SupT1^{BC1}, and SupT1^{C1} cells were stained with either CellTrace Violet (CTV) or CellTrace Far Red (CTR) before mixing of the separate cell lines in a 1:1 ratio and infection with HHV-6A$_{GS}$ and HHV-6B$_{Z29}$, respectively. After incubation for the indicated time, virus was removed by extensive washing, the cells were stained with the viability marker nIR, and the cells were fixed and analyzed using flow cytometry analysis. (A) Frequency of the differently stained populations obtained 6 h postinfection of the separate cell lines (one representative experiment). The populations shown represent living cells (gated using the viability marker nIR), without doublets (gated based on FSC-H versus FSC-A and SSC-H versus SSC-A). Cell-cell fusion is represented by the frequency of CTR+/CTV+ cells, presented in the upper right of the separate graphs. (B) Percentage of the CTR+/CTV+ cells obtained upon incubation with HHV-6A$_{GS}$ and HHV-6B$_{Z29}$ for the indicated time. The data represent the mean percentages ± SEM of sample values after subtraction of the representative mock, i.e., % sample − % mock, from three independent experiments.

mixed with either HHV-6A$_{GS}$ or HHV-6B$_{Z29}$. Double-positive cells (CTV/CTR) were quantified by flow cytometry at 2, 4, and 6 hpi (Fig. 7). This demonstrated that HHV-6B$_{Z29}$ but not HHV-6A$_{GS}$ gave rise to FFWO in cells expressing the C1 isoform of CD46. Taken together, this suggested that when HHV-6B$_{Z29}$ uses CD46 as a receptor for infection, it preferentially infects by cell-cell fusion dependent on the C1 isoform.

DISCUSSION

The expression of several isoforms of a receptor for pathogens raises the question of whether these isoforms are functionally different during infection. Earlier studies evaluating measles virus-induced syncytium formation using a CD46-transfected CHO cell model suggested that the C isoform provided better syncytium formation than the BC isoform (27). The C isoform was also more efficient in mediating measles virus-induced fusion in transfected Ltk mouse cells, although BC isoforms bound more measles virus (28). The significance of the B domain for the binding of pathogens was also observed for *N. gonorrhoeae* and *N. meningitidis* in CD46-transfected CHO cells (29). HHV-6A has been suggested to cause FFWO with all tested isoforms in CHO cells, with

FIG 6 Legend (Continued)
endocytosis inhibitors prior to and during infection with HHV-6A$_{GS}$ and HHV-6B$_{Z29}$. The bar graphs represent the level of U86 mRNA, shown as percentages of U86 mRNA in untreated cell lines, 7 hpi. The cells were treated with chloroquine (B) (0 to 50 μM), dynasore (C) (0 to 100 μM), and chlorpromazine (D) (0 to 25 μM). The viability of the cells is represented as percentages of living cells at the various inhibitor concentrations at 7 hpi, measured by flow cytometry. All data are presented as means ± SEM.

C and BC isoforms supporting FFWO more efficiently than A, B, or ABC isoforms (2). Although *in vitro* studies have shown that HHV-6A$_{GS}$ binds CD46 with significantly higher affinity than does HHV-6B$_{HST}$ (9), these studies do not account for a potential impact of CD46 isoforms on the cell surface. Previous observations from our laboratory suggested that cell lines with higher relative expression of the C isoforms were better infected with HHV-6B$_{PL1}$ than cell lines with low relative expression of the C isoforms (11). These studies strongly support the idea that CD46 contributes in an isoform-dependent manner to host cell susceptibility of HHV-6A and HHV-6B infections and possibly other pathogens as well.

In this study, we have demonstrated that HHV-6A$_{GS}$ preferentially uses the BC isoform in a T-cell model system, whereas HHV-6B$_{Z29}$ preferentially uses the C isoform. The exclusion of the B domain correlated with increased HHV-6B$_{Z29}$ infection by cell-cell fusion. To address the clathrin-mediated endocytosis pathway, we used the following inhibitors: chloroquine, dynasore, and chlorpromazine.

Chloroquine treatment resulted in enhanced transcription of HHV-6B mRNA in SupT1^{C1} (Fig. 6A). This paradoxical effect of chloroquine has previously been observed during other viral infections (30–35). Chloroquine treatment has previously been demonstrated to increase the infectivity of HIV by enhancing pH-independent fusion (32), supporting the idea that the increase in infectivity of HHV-6B$_{Z29}$ is facilitated by an increase in fusion at the plasma membrane.

Dynasore on the other hand was shown to change the HHV-6B gene expression in the opposite manner. Dynasore inhibits both clathrin and caveolin-dependent endocytosis by blocking the GTPase activity of dynamin (36, 37). Dynasore also affects dynamin-independent mechanisms, as it has been described to disperse the organization of lipid rafts, possibly by remodulating actin filaments and decreasing plasma membrane cholesterol (38). In particular, the latter effect may also affect cell-cell fusion, and even the lowest level of dynasore had an impact on infection by both viruses, although the effect was most pronounced on HHV-6A$_{GS}$. For C isoforms, the level of HHV-6B$_{Z29}$ viral transcripts appeared to increase at dynasore concentrations greater than 50 μM, which might be ascribed to off-target effects of dynasore.

The third inhibitor, chlorpromazine, has been described not to affect clathrin-independent virus entry mechanisms (39–42). The almost complete resistance toward chlorpromazine treatment and the increase in cell-cell fusion of HHV-6B$_{Z29}$-infected SupT1^{C1} cells compared with SupT1^{BC1} cells (Fig. 6 and 7) further support that C isoforms are capable of promoting another entry mechanism compared with BC isoforms. Thus, the differences between HHV-6A$_{GS}$ and HHV-6B$_{Z29}$ infection suggest separate entry mechanisms.

The results acquired with the inhibitors together with the FFWO assay (Fig. 7) support that C isoforms are capable of promoting another entry mechanism compared with BC isoforms. Structural analyses may help explain how distinctive entry mechanisms are supported by different CD46 isoforms. Simulated models of the predominantly expressed isoforms suggest that the 15 amino acids in the B domain make up two β strands. The exclusion of the B domain creates greater flexibility of CD46, which is speculated to create favorable conditions for triggering pH-independent membrane fusion or FFWO (43). A proposed model for infection with HHV-6A and HHV-6B is presented in Fig. 8.

Our data also demonstrated that *O*-linked glycosylations in the STP region were not required for infection by HHV-6A$_{GS}$. The predicted structure of SCR1-4 suggests a linear conformation of SCR1-3, followed by a bent arrangement of SCR4 (16). HHV-6A binds to SCR2 and SCR3, and the B domain may be critical for maintaining the proper structural conformation of CD46 upon HHV-6A binding, or it may simply be required to ensure the spatial distance of SCR2 and SCR3 from the membrane, to enable proper HHV-6A binding.

Viruses are capable of exploiting abundant cellular mechanisms to enhance survival and infection of specific host cells. The expression pattern of CD46 isoforms has been

proposed to be inheritable (44). Some individuals express primarily BC isoforms, others have equal amounts of BC and C isoforms, and approximately 6% of individuals mainly express the C isoforms (24, 44). Tissue-specific regulation of the expression pattern has also been demonstrated in the brain, kidney, salivary glands, and memory/effector T cells (23, 24, 45). By showing different entry mechanisms dependent on the expression of isoforms, our results suggest that the CD46 isoform phenotype matters for the susceptibility toward HHV-6A infection, and potentially HHV-6B infection in certain cells. We did not observe any significant difference between the two intracytoplasmic domains for HHV-6A and HHV-6B infectivity, a result that is in accordance with *in vivo* studies in transgenic CD46-expressing mice (46). However, the intracytoplasmic domains do exhibit distinctive signaling capacities in primary $CD4^+$ T cells, which is not supported by our cell system, and the Cyt1 domain is associated with the induction of autophagocytosis (47). These are factors that might influence virus infections in other cells or *in vivo*. Compared with other nonhuman cell systems, our human T-cell model system provides an advantage over other commonly used systems, since the infection may be influenced by other molecules and complexes not present in nonhuman cells (8). Nevertheless, we should caution that extrapolating these results to primary T cells, brain cells, and *in vivo* infections would require further studies.

Taken together, this study provides novel insight into the biological function of CD46 isoforms. Knowledge on the specific entry mechanisms of HHV-6A and HHV-6B is crucial for our understanding of the pathogenesis and development of novel treatment strategies. Importantly, our data suggest that the distinctive expression of CD46 isoforms modulates the entry mechanism of HHV-6A and HHV-6B. The intracellular defense against an invading pathogen is likely to depend on the entry mechanism. For example, the endosomal compartments contain Toll-like receptor 9, which may activate the immune response when sensing viral DNA. Whether or not HHV-6A and HHV-6B induce different types of immune response by virtue of their entry mechanisms remains to be determined.

MATERIALS AND METHODS

Cell lines, virus stock solutions, and infection. The human T-cell lymphoblast SupT1 cell line was kindly provided by the National Institutes of Health (NIH) AIDS Reagent Program (Division of AIDS, National Institute of Allergy and Infectious Diseases [NIAID], NIH, USA). The generation of CRISPR/Cas9 edited $SupT1^{\Delta CD46}$ is described by Schack et al. (8). The cell lines were maintained in RPMI 1640 (Sigma-Aldrich, USA), supplemented with 10% heat-inactivated fetal bovine serum (FBS) (Sigma-Aldrich), 2 mM GlutaMAX (Gibco, USA), 10 mM HEPES (Sigma-Aldrich), 100 U/mL penicillin, and 100 μg/mL streptomycin (complete medium). The cells were split 1:4 in fresh media 2 or 3 times a week. All cells were cultured at 37°C, 5% CO_2. HHV-$6A_{GS}$-infected HSB2 cells and HHV-$6B_{Z29}$-infected SupT1 cells were kindly provided by the HHV6 Foundation (48, 49). The HHV-$6A_{GS}$ and HHV-$6B_{Z29}$ were propagated in HSB2 and SupT1 cell lines, respectively, by supplying the infected cells with uninfected cells every 4 to 6 days. When the cytopathogenic effect (CPE) indicated a good infection, the cell suspension was centrifuged at 300 $\times$ *g* for 8 min. The supernatant was collected and stored on ice, and the cells were subjected to three -80°C freeze/thaw cycles to release viral particles. The cells were again centrifuged at 300 $\times$ *g* for 8 min in 1 mL virus supernatant, and the collected supernatants were pooled and spun at 3,200 $\times$ *g* for 1 h at 4°C, aliquoted, and stored at -80°C. HSB2 and SupT1 cells were infected with an aliquot of virus, and the viral titer was determined by a Reed-Muench assay (50). The multiplicity of infection (MOI) was 0.002 to 0.004 for HHV-$6A_{GS}$ and 0.01 for HHV-$6B_{Z29}$. In all experiments, the cells were adjusted to 0.5 $\times$ 10^6 cells/mL the day prior to infection. On the day of the infection, 2 $\times$ 10^6 cells/mL were incubated with virus stock solution.

Molecular cloning of CD46 isoforms. BC1, BC2, C1, and C2 isoforms were synthesized by GenScript (GenBank accession number NM_172351, amino acids 56 to 1531; NM_153826, amino acids 56 to 1438; NM_172352, amino acids 56 to 1486; and NM_172353, amino acids 56 to 1393). Using primers listed in Table 1, PCR products were amplified from a pcDNA3.1(+) vector containing each isoform. An internal ribosome entry site (IRES) element and a puromycin resistance gene (Puro) were similarly amplified from a pPBT/CMV-IRES-Puro vector. Four different lentiviral vectors were constructed by combining overlapping PCR products from BC1, BC2, C1, and C2 with IRES-Puro amplicons and a BamHI/XhoI-digested pCCL-WPS-PGK-puro-WHV vector using NEBuilder HIFI DNA assembly cloning kit (New England Biolabs, USA). Both of the vectors pCCL-WPS-PGK-puro-WHV and pPBT/CMV-IRES-Puro were kindly provided by J. Giehm Mikkelsen, Aarhus University, Denmark (51). The plasmids were transformed and cloned in NEB 5-alpha Competent *Escherichia coli*, and the sequences were verified by Sanger Sequencing (Eurofins Genomics, Germany).

Generation of STP mutants. Site-directed mutagenesis in the STP region of BC1 was performed with an approach similar to the one described above using the generated pCCL-$CD46^{BC1}$ vector as the template and a BamHI/ApaI-digested pCCL-WPS-PGK-puro-WHV vector as backbone. The generated STP

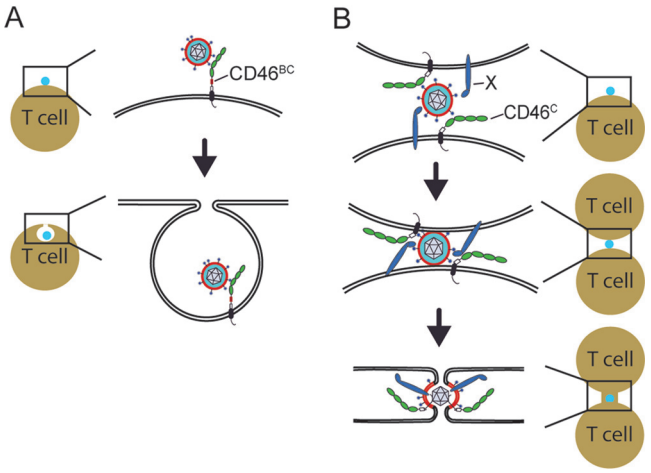

FIG 8 Models of the primary mechanisms of infection by HHV-6A and HHV-6B in SupT1 cells. (A) Interaction between HHV-6B and the SCR2 and SCR3 domains of $CD46^{BC}$ leads to endocytosis. Other molecules participating in this process are not shown. (B) $CD46^{C}$ has greater flexibility in the STP region and interacts with HHV-6B in closer proximity to the membrane. This may facilitate FFWO. HHV-6B has low avidity for CD46, and a postulated coreceptor X is indicated on the figure. The exact mechanisms for membrane fusion of HHV-6A and HHV-6B remain unknown.

mutants were named m1 to m6 and encompassed the following mutations: m1: S287A, S289A, S290A, and S294A; m2: T288A, T291A, and T292A; m3: S287A, T288A, S289A, S290A, T291A, T292A, and S294A; m4: S294A, S297A, S298A, and S300A; m5: S297A, S298A, and S300A; and m6: S287A, T288A, S289A, S290A, T291A, T292A, and S294A. The primers used are listed in Table 1.

Generation of SupT1 cell lines stably expressing CD46 isoforms. Lentiviral particles were produced by cotransfecting HEK293T cells with 1 μg pRSV-REV, 2 μg pMD.2G, 2 μg pMDLg/p-RRE, and 3 μg pCCL-WPS-PGK-CD46-puro-WHV vector using FuGENE HD transfection reagent (Promega Corporation, USA). At 24 h prior to transfection, 8×10^6 HEK293T cells were plated to approximately 40 to 50% confluence. Transfection was done according to the manufacturer's protocol, and the culture medium was collected at 48 and 72 h posttransfection. The collected medium was filtered through a 450-nm filter and concentrated using 20% sucrose solution and 25,000 $\times$ *g*, 4°C, and 2 h ultracentrifugation. The lentiviral particles were resuspended in phosphate-buffered saline (PBS) using three cycles of vortexing (15 s) and incubation at 0°C (2 min), aliquoted, and stored at −80°C. $SupT1^{\Delta CD46}$ cells were adjusted to 0.5×10^6 cells/mL 24 h prior to transduction. Real-time PCR on integrated lentiviral DNA was performed as previously described (52), with some modifications. Our analysis was based on the use of Brilliant II SYBR green quantitative PCR (qPCR) master mix (Agilent Technologies, USA), SupT1 cells and primers specific against the WPRE sequence in the lentiviral vector, and the albumin gene in cells (Table 1), allowing an estimation of the lentiviral titer. For the generation of stable cell lines, $SupT1^{\Delta CD46}$ cells at a concentration of 0.5×10^6 cells/mL were transduced with different amounts of lentivirus in the presence of 25 μg/mL protamine sulfate (Sigma-Aldrich) in a 6-well plate. 24 h postransduction, the cells were selected with 2 μg/mL puromycin (Gibco) for 14 days. The established cell lines were analyzed using flow cytometry, allowing an evaluation of the CD46 expression and a selection of cell lines with a similar CD46 expression level. The stability of CD46 expression was verified on a regular basis and always before virus infection, using anti-CD46 antibody clone MEM-258 (Sigma-Aldrich), recognizing SCR4 as described below. To validate the results obtained with clone MEM-258, we also performed analyses with anti-CD46 antibody clone M177 (Thermo Fisher Scientific, USA), recognizing SCR2 of CD46. In order to produce a $SupT1^{C1/BC1}$ cell line, $SupT1^{C1.1}$ was transduced with different amounts of BC1 lentiviral particles. The total expression of CD46 was analyzed using flow cytometry as described below, whereas the distribution of the separate isoforms was analyzed using qPCR as previously described (23). Both flow cytometry and qPCR were performed at the same time as the cells were infected with $HHV\text{-}6A_{GS}$ and $HHV\text{-}6B_{Z29}$.

Flow cytometry analysis. For flow cytometry analysis 0.3 to 0.5×10^6 cells were washed in PBS supplemented with 2% FBS. The cells were incubated with 5 μl CD46 antibody (Ab) conjugated with phycoerythrin (PE) (MEM-258, Sigma-Aldrich) and 1:100 LIVE/DEAD fixable Near-IR (nIR) (Thermo Fisher Scientific) in PBS supplemented with 2% FBS in a total volume of 50 μl for 30 min at 4°C. The cells were washed twice with PBS supplemented with 2% FBS, resuspended in 0.99% paraformaldehyde in PBS, and analyzed the same day on a Novocyte flow cytometer (ACEA Bioscience, USA) or a Novocyte Quanteon flow cytometer (ACEA Bioscience). The data were analyzed using FlowJo software, version 10. To determine the binding of virus, the cells were indirectly stained with Ab against gp60/110. Briefly, the cells were incubated 30 min in complete medium containing 0.1% sodium azide to stop cellular uptake of virus. The cells were centrifuged and resuspended in HHV-6A containing 0.1% sodium azide and incubated for 2 and 4 h. The cells were washed three times with PBS supplemented with 2% FBS and stained with either 5 μl mouse monoclonal gp60/110 Ab (Millipore, USA) or 5 μl isotype IgG2b Ab control (MOPC-141, Sigma-Aldrich) for 30 min at 4°C. All samples were stained with 0.6 μl goat anti-mouse IgG1 secondary Ab conjugated with phycoerythrin (PE) (Thermo Fisher Scientific) and analyzed by flow cytometry as described above.

TABLE 1 Cloning primers[a]

Target	Oligonucleotides	Sequence (5′ to 3′)
CD46	Forward	GGGCCTTTCGACCTCTAGCGGGATCCATCTACCATTGTTGCGTCCCATATCTGG
	Reverse	TTACTTGTACGAAGCCACATTGCAATATTAGCTAAGC
IRES-Puro	Forward	CAATGTGGCTTCGTACAAGTAAAGCATAGCGGCCG
	Reverse	AGGTTGATTATCGGAATTCCCTCGAGGGGGATCTTCAGGCACCGGGCTTGCG
STP m1	Forward	GGGCCTTTCGACCTCTAGCGGGATCCATCTACCATTGTTGCGTCCCATATCTGG
	Reverse	CTTTTGTAGTGGCAGCAGTCGCCACTTTAAGACACTTTGGAACTGG
IRES-Puro 1	Forward	ACTGCTGCCACTACAAAAGCTCCAGCGTCCAGTGCCTCA
	Reverse	GAAGACAGGGCCAGGTTTCCGGGCCCTCACATTGCCAAAAGACG
STP m2	Forward	GGGCCTTTCGACCTCTAGCGGGATCCATCTACCATTGTTGCGTCCCATATCTGG
	Reverse	TGCAGCGGAAGAAGCCGACACTTTAAGACACTTTGGAAC
IRES-Puro 2	Forward	GTCGGCTTCTTCCGCTGCAAAATCTCCAGCGTCCAGT
	Reverse	GAAGACAGGGCCAGGTTTCCGGGCCCTCACATTGCCAAAAGACG
STP m3	Forward	GGGCCTTTCGACCTCTAGCGGGATCCATCTACCATTGTTGCGTCCCATATCTGG
	Reverse	CTTTTGCAGCGGCAGCAGCCGCCACTTTAAGACACTTTGGAACTGG
IRES-Puro 3	Forward	GCTGCTGCCGCTGCAAAAGCTCCAGCGTCCAGTGCCTCA
	Reverse	GAAGACAGGGCCAGGTTTCCGGGCCCTCACATTGCCAAAAGACG
STP m4	Forward	GGGCCTTTCGACCTCTAGCGGGATCCATCTACCATTGTTGCGTCCCATATCTGG
	Reverse	GCGGCAGCGGCCGCTGGAGCTTTTGTAGTGGAAGAAGTCGAC
IRES-Puro 4	Forward	CTCCAGCGGCCGCTGCCGCAGGTCCTAGGCCTACTTAC
	Reverse	GAAGACAGGGCCAGGTTTCCGGGCCCTCACATTGCCAAAAGACG
STP m5	Forward	GGGCCTTTCGACCTCTAGCGGGATCCATCTACCATTGTTGCGTCCCATATCTGG
	Reverse	GCGGCAGCGGCCGCTGGAGATTTTGTAGTGG
IRES-Puro 5	Forward	CTCCAGCGGCCGCTGCCGCAGGTCCTAGGCCTACTTAC
	Reverse	GAAGACAGGGCCAGGTTTCCGGGCCCTCACATTGCCAAAAGACG
STP m6	Forward	GGGCCTTTCGACCTCTAGCGGGATCCATCTACCATTGTTGCGTCCCATATCTGG
	Reverse	GCGGCAGCGGCCGCTGGAGCTTTTGCAGCG
IRES-Puro 6	Forward	CTCCAGCGGCCGCTGCCGCAGGTCCTAGGCCTACTTAC
	Reverse	GAAGACAGGGCCAGGTTTCCGGGCCCTCACATTGCCAAAAGACG

[a]IRES, internal ribosome entry site; STP, serine-threonine-proline-rich region.

RNA purification and cDNA synthesis. Total RNA was isolated using Nucleospin RNA columns (Macherey-Nagel, Germany) according to the manufacturer's instructions. Infected cells were washed three times in PBS prior to RNA isolation. The RNA was eluted using 30 μl RNase-free water, and the total amount of RNA in each sample was measured with a NanoDrop 1000 (Thermo Fisher Scientific). An equal amount of total RNA for each experiment (500 to 1,000 ng) was used for cDNA synthesis using a QuantiTect reverse transcription kit (Qiagen, Germany) according to the manufacturer's protocol. The cDNA was diluted 1:5 in RNase-free water before real-time PCR analysis.

DNA extraction from cell supernatant. The cells were incubated with virus stock solution at a concentration of 2×10^6 cells/mL for 4 h. Afterwards, the cells were washed twice in complete medium, before resuspension in fresh medium and a following incubation at a concentration of 1×10^6 cells/mL in a 48-well plate at 37°C, 5% CO_2. The cells were pelleted at 400 $\times$ *g* for 8 min. DNA was extracted from 200 μl supernatant using high pure viral nucleic acid kit (Roche Diagnostics, Germany) according to the manufacturer's protocol. A standard curve was used to calculate the amount of DNA, and real-time PCR analysis was performed as described below.

Real-time PCR. Real-time PCR analyses for expression of viral nucleic acids were performed using PowerUp SYBR green master mix (Thermo Fisher Scientific) and a QuantStudio 5 real-time PCR system (Applied Biosystems, USA). All primers were used at a final concentration of 500 nM. A list of primers is included in Table 2. Viral RNA transcripts were normalized to human peptidylpropyl isomerase B (PPIB), and statistical analyses were performed on $\Delta\Delta$CT values using the Mann-Whitney test and GraphPad Prism version 8. All real-time PCR analyses were performed in technical triplicate. Determination of CD46 isoform expression was performed as previously described (23).

Cell lysis and Western blotting. For Western blotting, 2×10^6 cells were washed twice in cold PBS and lysed according to the manufacturer's protocol using 100 μl cell lysis buffer (product number 9803, Cell Signaling Technology, USA) supplemented with 150 μl stock solution of complete mini protease inhibitor diluted in lysis buffer (Roche Diagnostics, USA), 5 mM sodium fluoride (NaF), and 1 mM phenylmethanesulfonyl fluoride (PMSF). The protein concentration in the collected supernatants was determined by the Bradford method. The CD46 migration pattern was analyzed on a 10% Bis-Tris gel (Bio-Rad, USA) with XT MOPS running buffer (Bio-Rad) according to the manufacturer's protocol. The proteins were transferred to a Trans-Blot Turbo 0.2 μm polyvinylidene difluoride (PVDF) membrane by the Trans-Blot Turbo Transfer System (Bio-Rad) and blocked in 5% skimmed milk (Sigma-Aldrich) in Tris-buffered saline (TBS) with 0.1% Tween 20 (Sigma-Aldrich) for 1 h. For detection, the membrane was incubated overnight with 1:5,000 mouse anti-CD46 antibody (clone EPR4014; Abcam, UK) at 4°C, followed by extensive washing in TBS with 0.1% Tween 20. The membrane was incubated with horseradish peroxidase (HRP)-conjugated polyclonal rabbit anti-mouse IgG (1:2,000) (Dako, Denmark) for 1 h at 20°C before development using SuperSignal West Pico PLUS chemiluminescent substrate (Thermo Fisher Scientific) and a ChemiDoc imaging system

TABLE 2 Real-time PCR primers

Target	Oligonucleotides	Sequence (5′ to 3′)	Amplicon size (bp)
U81 HHV-6A[a]	Forward	CGTTGTCAGGGGGGGAAAAAT	108
	Reverse	GCGGCTTGGCCTTCGGTA	
U86 HHV-6A	Forward	ATGGGCGTAGCGGCGTAA	119
	Reverse	CAACTACAAAAACAAGGACCGCAAGAA	
U7 HHV-6A	Forward	CGCAAGCCCGGAGAACTGATT	338/233[b]
	Reverse	AGACTTTTTGCGGACTGCGGT	
U23 HHV-6A	Forward	ATCACCCTTGACCGTCGGAA	168
	Reverse	GCGAATTCTGAAACGTGGGG	
U81 HHV-6B	Forward	TCAGCATTCACTCTTCGGCA	179
	Reverse	CATCGGTGGGTTTGCACAAA	
U86 HHV-6B	Forward	AAAGGACTGGAGTCGAGCTGCA	204
	Reverse	ATGTCCAACATACCTTCCCCTCAAACTT	
U7 HHV-6B	Forward	ACGACAAACCTGCTGGTAGCG	291/200[b]
	Reverse	GGATGTTGAATGGGGAGTTGCCC	
U23 HHV-6B	Forward	GAATGCCCCGACAAAACTAATCCCG	252
	Reverse	GATGAGGCGCAGGATATTGAGACGT	
PPIB	Forward	CAACGCAGGCAAAGACACCAAC	156
	Reverse	GGTTTATCCCGGCTGTCTGTCTTG	

[a]HHV, human herpesvirus; PPIB, peptidylpropyl isomerase B.
[b]Length of amplified DNA or cDNA (from spliced RNA).

(Bio-Rad). The membrane was stripped and reincubated with rabbit anti-glyceraldehyde-3-phosphate dehydrogenase (GAPDH) (1:1,000) (ab9485, Abcam) and an HRP-conjugated polyclonal swine anti-rabbit IgG (1:2,000) (Dako).

Inhibition of clathrin-mediated endocytosis. One hour before infection, 2×10^6 cells/mL were centrifuged ($400 \times g$, 6 min) and resuspended in stock solutions of chloroquine (50 mM in water), dynasore (10 mM in DMSO), chlorpromazine (10 mM in water) (inhibitors from Sigma-Aldrich), or complete medium with or without DMSO control. The cells were centrifuged once more and incubated with virus supplemented with inhibitors or control medium in a 48-well plate at 37°C and 5% CO_2. Thus, the presence of inhibitors was held constant before and during incubation with virus. After 8 h, 0.32×10^6 cells were washed once with PBS, stained with 1:100 dilution of nIR for 30 min at 4°C, washed again, resuspended in 0.99% paraformaldehyde in PBS, and analyzed by flow cytometry. In a parallel experimental setup, the cells were washed three times in PBS and used for purification of RNA and real-time PCR analysis of viral mRNA transcripts.

FFWO analysis. SupT1 cells were stained with either 5 μM CellTrace Violet (CTV) (Thermo Fisher Scientific) or 1 μM CellTrace Far Red (CTR) for 20 min, following the manufacturer's instruction. Free stain was removed by washing the cells for 5 min in culture medium with a volume 5 times the initial staining volume. The cells were centrifuged ($300 \times g$, 8 min) and resuspended in fresh culture medium. The CTV- and CTR-stained cells were mixed 1:1, pelleted, and resuspended in complete medium, HHV-$6A_{GS}$, or HHV-$6B_{Z29}$ stock solution. The cells were incubated in a 48-well plate for 2, 4, and 6 h. Following incubation, the cells were washed twice in PBS supplemented with 2% FCS and stained with nIR (1:100 dilution). The cells were washed once before fixation in 0.99% paraformaldehyde in PBS. The cells were analyzed on a Novocyte flow cytometer (ACEA Bioscience).

Data availability. The raw data will be made available upon request.

ACKNOWLEDGMENTS

We thank the staff at the FACS Core Facility, Aarhus University, Denmark, for help and advice on FACS and flow cytometry analyses. We are grateful to the NIH AIDS Reagent Program, Division of AIDS, NIAID, NIH, for providing cell lines. Also, we thank D. Ablashi and K. Loomis and the HHV-6 Foundation for providing HHV-$6A_{GS}$ in HSB2 cells and HHV-$6B_{Z29}$ in SupT1 cells and J. Giehm Mikkelsen for providing expression vectors.

This work was supported by grants from the Independent Research Fund Denmark (P.H.), the Nyegaard Foundation (P.H.), the Riisfort Foundation (P.H., V.R.S.), the Hoerslev Foundation (V.R.S.), and the Graduate School of Health (L.S.R.).

REFERENCES

1. Sobhy H. 2017. A comparative review of viral entry and attachment during large and giant dsDNA virus infections. Arch Virol 162:3567–3585. https://doi.org/10.1007/s00705-017-3497-8.
2. Mori Y, Seya T, Huang HL, Akkapaiboon P, Dhepakson P, Yamanishi K. 2002. Human herpesvirus 6 variant A but not variant B induces fusion from without in a variety of human cells through a human herpesvirus 6 entry receptor, CD46. J Virol 76:6750–6761. https://doi.org/10.1128/jvi.76.13.6750-6761.2002.
3. Cirone M, Zompetta C, Angeloni A, Ablashi DV, Salahuddin SZ, Pavan A, Torrisi MR, Frati L, Faggioni A. 1992. Infection by human herpesvirus 6 (HHV-6) of human lymphoid T cells occurs through an endocytic pathway. AIDS Res Hum Retroviruses 8:2031–2037. https://doi.org/10.1089/aid.1992.8.2031.
4. Tang H, Kawabata A, Takemoto M, Yamanishi K, Mori Y. 2008. Human herpesvirus-6 infection induces the reorganization of membrane microdomains in

target cells, which are required for virus entry. Virology 378:265–271. https://doi.org/10.1016/j.virol.2008.05.028.
5. Pedersen SM, Hollsberg P. 2006. Complexities in human herpesvirus-6A and -6B binding to host cells. Virology 356:1–3. https://doi.org/10.1016/j.virol.2006.07.028.
6. Santoro F, Kennedy PE, Locatelli G, Malnati MS, Berger EA, Lusso P. 1999. CD46 is a cellular receptor for human herpesvirus 6. Cell 99:817–827. https://doi.org/10.1016/s0092-8674(00)81678-5.
7. Nishimura M, Mori Y. 2019. Entry of betaherpesviruses. Adv Virus Res 104:283–312. https://doi.org/10.1016/bs.aivir.2019.05.005.
8. Schack VR, Rossen LS, Ekebjærg CC, Thuesen KKH, Bundgaard B, Höllsberg P. 2021. The tetraspanin protein CD9 modulates infection with human herpesvirus 6A and 6B in a CD46-dependent manner. J Virol 95:e02259-20. https://doi.org/10.1128/JVI.02259-20.
9. Mori Y, Akkapaiboon P, Yonemoto S, Koike M, Takemoto M, Sadaoka T, Sasamoto Y, Konishi S, Uchiyama Y, Yamanishi K. 2004. Discovery of a second form of tripartite complex containing gH-gL of human herpesvirus 6 and observations on CD46. J Virol 78:4609–4616. https://doi.org/10.1128/jvi.78.9.4609-4616.2004.
10. Tang H, Serada S, Kawabata A, Ota M, Hayashi E, Naka T, Yamanishi K, Mori Y. 2013. CD134 is a cellular receptor specific for human herpesvirus-6B entry. Proc Natl Acad Sci U S A 110:9096–9099. https://doi.org/10.1073/pnas.1305187110.
11. Hansen AS, Bundgaard BB, Biltoft M, Rossen LS, Hollsberg P. 2017. Divergent tropism of HHV-6AGS and HHV-6BPL1 in T cells expressing different CD46 isoform patterns. Virology 502:160–170. https://doi.org/10.1016/j.virol.2016.12.027.
12. Kurita-Taniguchi M, Hazeki K, Murabayashi N, Fukui A, Tsuji S, Matsumoto M, Toyoshima K, Seya T. 2002. Molecular assembly of CD46 with CD9, alpha3-beta1 integrin and protein tyrosine phosphatase SHP-1 in human macrophages through differentiation by GM-CSF. Mol Immunol 38:689–700. https://doi.org/10.1016/s0161-5890(01)00100-6.
13. Florin L, Lang T. 2018. Tetraspanin assemblies in virus infection. Front Immunol 9:1140. https://doi.org/10.3389/fimmu.2018.01140.
14. Monk PN, Partridge LJ. 2012. Tetraspanins: gateways for infection. Infect Disord Drug Targets 12:4–17. https://doi.org/10.2174/187152612798994957.
15. Liszewski MK, Atkinson JP. 2021. Membrane cofactor protein (MCP; CD46): deficiency states and pathogen connections. Curr Opin Immunol 72:126–134. https://doi.org/10.1016/j.coi.2021.04.005.
16. Persson BD, Schmitz NB, Santiago C, Zocher G, Larvie M, Scheu U, Casasnovas JM, Stehle T. 2010. Structure of the extracellular portion of CD46 provides insights into its interactions with complement proteins and pathogens. PLoS Pathog 6:e1001122. https://doi.org/10.1371/journal.ppat.1001122.
17. Greenstone HL, Santoro F, Lusso P, Berger EA. 2002. Human herpesvirus 6 and measles virus employ distinct CD46 domains for receptor function. J Biol Chem 277:39112–39118. https://doi.org/10.1074/jbc.M206488200.
18. Yang X, Coulombe-Huntington J, Kang S, Sheynkman GM, Hao T, Richardson A, Sun S, Yang F, Shen YA, Murray RR, Spirohn K, Begg BE, Duran-Frigola M, MacWilliams A, Pevzner SJ, Zhong Q, Trigg SA, Tam S, Ghamsari L, Sahni N, Yi S, Rodriguez MD, Balcha D, Tan G, Costanzo M, Andrews B, Boone C, Zhou XJ, Salehi-Ashtiani K, Charloteaux B, Chen AA, Calderwood MA, Aloy P, Roth FP, Hill DE, Iakoucheva LM, Xia Y, Vidal M. 2016. Widespread expansion of protein interaction capabilities by alternative splicing. Cell 164:805–817. https://doi.org/10.1016/j.cell.2016.01.029.
19. Cardone J, Le Friec G, Vantourout P, Roberts A, Fuchs A, Jackson I, Suddason T, Lord G, Atkinson JP, Cope A, Hayday A, Kemper C. 2010. Complement regulator CD46 temporally regulates cytokine production by conventional and unconventional T cells. Nat Immunol 11:862–871. https://doi.org/10.1038/ni.1917.
20. Ni Choileain S, Weyand NJ, Neumann C, Thomas J, So M, Astier AL. 2011. The dynamic processing of CD46 intracellular domains provides a molecular rheostat for T cell activation. PLoS One 6:e16287. https://doi.org/10.1371/journal.pone.0016287.
21. Hansen AS, Biltoft M, Bundgaard B, Bohn AB, Moller BK, Hollsberg P. 2019. CD46 activation induces distinct CXCL-10 response in monocytes and monocyte-derived dendritic cells. Cytokine 113:466–469. https://doi.org/10.1016/j.cyto.2018.06.030.
22. Post TW, Liszewski MK, Adams EM, Tedja I, Miller EA, Atkinson JP. 1991. Membrane cofactor protein of the complement system: alternative splicing of serine/threonine/proline-rich exons and cytoplasmic tails produces multiple isoforms that correlate with protein phenotype. J Exp Med 174:93–102. https://doi.org/10.1084/jem.174.1.93.
23. Hansen AS, Bundgaard BB, Moller BK, Hollsberg P. 2016. Non-random pairing of CD46 isoforms with skewing towards BC2 and C2 in activated and memory/effector T cells. Sci Rep 6:35406. https://doi.org/10.1038/srep35406.
24. Johnstone RW, Russell SM, Loveland BE, McKenzie IF. 1993. Polymorphic expression of CD46 protein isoforms due to tissue-specific RNA splicing. Mol Immunol 30:1231–1241. https://doi.org/10.1016/0161-5890(93)90038-d.
25. Kallstrom H, Blackmer Gill D, Albiger B, Liszewski MK, Atkinson JP, Jonsson AB. 2001. Attachment of *Neisseria gonorrhoeae* to the cellular pilus receptor CD46: identification of domains important for bacterial adherence. Cell Microbiol 3:133–143. https://doi.org/10.1046/j.1462-5822.2001.00095.x.
26. Oster B, Hollsberg P. 2002. Viral gene expression patterns in human herpesvirus 6B-infected T cells. J Virol 76:7578–7586. https://doi.org/10.1128/JVI.76.15.7578-7586.2002.
27. Iwata K, Seya T, Ueda S, Ariga H, Nagasawa S. 1994. Modulation of complement regulatory function and measles virus receptor function by the serine-threonine-rich domains of membrane cofactor protein (CD46). Biochem J 304:169–175. https://doi.org/10.1042/bj3040169.
28. Buchholz CJ, Gerlier D, Hu A, Cathomen T, Liszewski MK, Atkinson JP, Cattaneo R. 1996. Selective expression of a subset of measles virus receptor-competent CD46 isoforms in human brain. Virology 217:349–355. https://doi.org/10.1006/viro.1996.0122.
29. Kallstrom H, Liszewski MK, Atkinson JP, Jonsson AB. 1997. Membrane cofactor protein (MCP or CD46) is a cellular pilus receptor for pathogenic *Neisseria*. Mol Microbiol 25:639–647. https://doi.org/10.1046/j.1365-2958.1997.4841857.x.
30. Laliberte JP, Weisberg AS, Moss B. 2011. The membrane fusion step of vaccinia virus entry is cooperatively mediated by multiple viral proteins and host cell components. PLoS Pathog 7:e1002446. https://doi.org/10.1371/journal.ppat.1002446.
31. Fredericksen BL, Wei BL, Yao J, Luo T, Garcia JV. 2002. Inhibition of endosomal/lysosomal degradation increases the infectivity of human immunodeficiency virus. J Virol 76:11440–11446. https://doi.org/10.1128/jvi.76.22.11440-11446.2002.
32. Schaeffer E, Soros VB, Greene WC. 2004. Compensatory link between fusion and endocytosis of human immunodeficiency virus type 1 in human CD4 T lymphocytes. J Virol 78:1375–1383. https://doi.org/10.1128/jvi.78.3.1375-1383.2004.
33. Richetta C, Gregoire IP, Verlhac P, Azocar O, Baguet J, Flacher M, Tangy F, Rabourdin-Combe C, Faure M. 2013. Sustained autophagy contributes to measles virus infectivity. PLoS Pathog 9:e1003599. https://doi.org/10.1371/journal.ppat.1003599.
34. Wu L, Dai J, Zhao X, Chen Y, Wang G, Li K. 2015. Chloroquine enhances replication of influenza A virus A/WSN/33 (H1N1) in dose-, time-, and MOI-dependent manners in human lung epithelial cells A549. J Med Virol 87:1096–1103. https://doi.org/10.1002/jmv.24135.
35. Li X, Burton EM, Bhaduri-McIntosh S. 2017. Chloroquine triggers Epstein-Barr virus replication through phosphorylation of KAP1/TRIM28 in Burkitt lymphoma cells. PLoS Pathog 13:e1006249. https://doi.org/10.1371/journal.ppat.1006249.
36. Macia E, Ehrlich M, Massol R, Boucrot E, Brunner C, Kirchhausen T. 2006. Dynasore, a cell-permeable inhibitor of dynamin. Dev Cell 10:839–850. https://doi.org/10.1016/j.devcel.2006.04.002.
37. Marks B, Stowell MH, Vallis Y, Mills IG, Gibson A, Hopkins CR, McMahon HT. 2001. GTPase activity of dynamin and resulting conformation change are essential for endocytosis. Nature 410:231–235. https://doi.org/10.1038/35065645.
38. Preta G, Cronin JG, Sheldon IM. 2015. Dynasore – not just a dynamin inhibitor. Cell Commun Signal 13:24. https://doi.org/10.1186/s12964-015-0102-1.
39. Sun X, Yau VK, Briggs BJ, Whittaker GR. 2005. Role of clathrin-mediated endocytosis during vesicular stomatitis virus entry into host cells. Virology 338:53–60. https://doi.org/10.1016/j.virol.2005.05.006.
40. Blanchard E, Belouzard S, Goueslain L, Wakita T, Dubuisson J, Wychowski C, Rouille Y. 2006. Hepatitis C virus entry depends on clathrin-mediated endocytosis. J Virol 80:6964–6972. https://doi.org/10.1128/JVI.00024-06.
41. Miller N, Hutt-Fletcher LM. 1992. Epstein-Barr virus enters B cells and epithelial cells by different routes. J Virol 66:3409–3414. https://doi.org/10.1128/JVI.66.6.3409-3414.1992.
42. Zhao T, Cui L, Yu X, Zhang Z, Shen X, Hua X. 2019. Entry of sapelovirus into IPEC-J2 cells is dependent on caveolae-mediated endocytosis. Virol J 16:37. https://doi.org/10.1186/s12985-019-1144-6.
43. Haralambieva IH, Ovsyannikova IG, Kennedy RB, Larrabee BR, Zimmermann MT, Grill DE, Schaid DJ, Poland GA. 2017. Genome-wide associations of CD46 and IFI44L genetic variants with neutralizing antibody response to measles vaccine. Hum Genet 136:421–435. https://doi.org/10.1007/s00439-017-1768-9.

44. Wilton AN, Johnstone RW, McKenzie IF, Purcell DF. 1992. Strong associations between RFLP and protein polymorphisms for CD46. Immunogenetics 36:79–85. https://doi.org/10.1007/BF00215283.
45. Russell SM, Sparrow RL, McKenzie IF, Purcell DF. 1992. Tissue-specific and allelic expression of the complement regulator CD46 is controlled by alternative splicing. Eur J Immunol 22:1513–1518. https://doi.org/10.1002/eji.1830220625.
46. Reynaud JM, Jegou JF, Welsch JC, Horvat B. 2014. Human herpesvirus 6A infection in CD46 transgenic mice: viral persistence in the brain and increased production of proinflammatory chemokines via Toll-like receptor 9. J Virol 88:5421–5436. https://doi.org/10.1128/JVI.03763-13.
47. Joubert PE, Meiffren G, Gregoire IP, Pontini G, Richetta C, Flacher M, Azocar O, Vidalain PO, Vidal M, Lotteau V, Codogno P, Rabourdin-Combe C, Faure M. 2009. Autophagy induction by the pathogen receptor CD46. Cell Host Microbe 6:354–366. https://doi.org/10.1016/j.chom.2009.09.006.
48. Salahuddin SZ, Ablashi DV, Markham PD, Josephs SF, Sturzenegger S, Kaplan M, Halligan G, Biberfeld P, Wong-Staal F, Kramarsky B. 1986. Isolation of a new virus, HBLV, in patients with lymphoproliferative disorders. Science 234:596–601. https://doi.org/10.1126/science.2876520.
49. Adams RA, Flowers A, Davis BJ. 1968. Direct implantation and serial transplantation of human acute lymphoblastic leukemia in hamsters, SB-2. Cancer Res 28:1121–1125.
50. Reed LJ, Muench H. 1938. A simple method of estimating fifty per cent endpoints. Am J Hyg 27:493–497. https://doi.org/10.1093/oxfordjournals.aje.a118408.
51. Moldt B, Staunstrup NH, Jakobsen M, Yanez-Munoz RJ, Mikkelsen JG. 2008. Genomic insertion of lentiviral DNA circles directed by the yeast Flp recombinase. BMC Biotechnol 8:60. https://doi.org/10.1186/1472-6750-8-60.
52. Bak RO, Hollensen AK, Primo MN, Sorensen CD, Mikkelsen JG. 2013. Potent microRNA suppression by RNA Pol II-transcribed "tough decoy" inhibitors. RNA 19:280–293. https://doi.org/10.1261/rna.034850.112.